Pharmacokinetic Model for Procaine in Humans during and following Intravenous Infusion

RANDOLPH H. SMITH *ˣ, DANIEL H. HUNT ‡, ASTRIDE B. SEIFEN *, ALFREDO FERRARI *, and DOLA S. THOMPSON *

Abstract □ A multicompartment pharmacokinetic model is presented to describe procaine distribution in humans during and following intravenous infusion. The model, based on a general perfusion model, relates individual characteristics such as sex, age, weight, height, infusion rate and duration, and hematocrit to general parameters such as drug metabolism, protein binding, ion-trapping effects, and tissue-plasma distribution coefficients to provide an individualized distribution prediction. Experimentally observed kinetics of blood procaine levels collected during intravenous procaine infusion as an adjunct to surgical anesthesia and blood lidocaine levels obtained from the literature compared very well with the model simulation.

Keyphrases □ Pharmacokinetics—procaine in humans, intravenous infusion, drug interactions □ Procaine—pharmacokinetics, intravenous infusion, humans, drug interactions □ Local anesthetics—procaine, pharmacokinetics, intravenous infusion, humans, drug interactions □ Models, pharmacokinetic—procaine, intravenous infusion, humans, drug interactions

Local anesthetics are given intravenously for various clinical purposes. Intravenous procaine is now being studied as a supplement or adjunct to general anesthesia, whereas in the past it has been used for local anesthesia, for intravenous regional anesthesia, and in cardiac arrhythmia treatment.

In these clinical applications, there are potential dangers to the patient such as cardiovascular depression and central nervous system toxicity. The ability to predict drug concentrations in various body organs as the result of intravenous infusion rates could aid the clinician's choice of an infusion rate and thereby offer additional safety in drug administration. Additionally, the clinical application of intravenous local anesthetics is usually simultaneous with the application of other drugs. Therefore, a potential for interaction between the various drugs exists. These interactions can change significantly the degree of pharmacological action expressed by the drugs individually.

This project was undertaken in order to describe and simulate the pharmacokinetics of intravenous procaine used as an adjuvant drug for surgical anesthesia.

BACKGROUND

In traditional pharmacokinetic studies, the drug concentration in the blood is used as an index because the clinical sampling procedure for blood is easier and more convenient than the sampling of other tissues and fluids. The traditional pharmacokinetic approach (1–3) is to correlate the drug concentration in blood data by using one or several exponential terms, with each exponential term representing a compartment, to describe the data. The distribution volumes, rate constant, etc., in the pharmacokinetic model are determined from the parameters of the exponential equation describing the drug concentration in blood (4).

The traditional approach utilizing the pharmacokinetic distribution based on these data alone may not provide sufficient information for adequate therapy when such drugs as ultrashort-acting barbiturates, some cardiovascular drugs, especially cancer chemotherapeutic agents, and local anesthetics are employed. An additional knowledge of the drug distribution in various organs and tissues as well as in the blood may be necessary to provide optimal drug concentrations in areas targeted for treatment without undue risk.

Previous investigators (5–7) developed an entirely different approach to pharmacokinetic modeling to make a priori prediction of drug distributions in the body. Included were parameters such as blood flow rates, lipid solubility, protein binding, and metabolism based on in vitro studies of well-documented physiological parameters. The model described here is an extension of this perfusion model approach with additional parameters that improve the scaling to different body sizes based on fat-free proportions as well as account for erythrocyte ion trapping.

EXPERIMENTAL

Arterial blood samples were collected from human volunteers undergoing intravenous procaine infusion as an adjuvant to surgical anesthesia along with thiamylal and nitrous oxide. These samples were collected before, during, and after the infusion. An inhibitor of plasma butyrylcholinesterase (pseudocholinesterase) was added to preserve the procaine for analysis. A flame-ionization GLC technique (8) was used to determine the blood concentrations. Additional parameters such as age, weight, height, sex, hematocrit, and other drugs administered were collected for use in the simulation. The exact infusion rates and duration were determined also.

THEORETICAL

The model can be thought of as an interactive blood–drug–tissue system. To describe such a system, previous investigators (5–7) used a four-compartment model with the body divided into the blood pool, the viscera, the lean tissue, and the adipose tissue. They utilized this scheme to describe the pharmacokinetics of several drugs such as thiopental and methotrexate.

This study of clinical intravenous procaine use focuses on the drug concentration in the brain because of anesthetic and potential convulsive effects. The blood pool was divided into separate arterial and venous pools with a lung compartment added to provide a mixing and time delay between the arterial and venous pools since procaine is hydrolyzed very rapidly by the plasma cholinesterases. Additional compartments were added to describe procaine metabolism in the liver and the ion-trapping effect due to the lower pH within the GI tract. The model (Fig. 1) contains nine compartments and adequately describes intravenous procaine pharmacokinetics, although consideration could be given to separating the blood from tissue for the highly perfused organs due to borderline adherence to the basic assumption of instantaneous mixing or flow-limitation of the system.

Each compartment equation describes a material (drug mass) balance between the incoming and outgoing drug rates. For example, blood flowing into a compartment transports an amount of drug at an incoming rate equal to the volume flow times the total concentration. Summation of all incoming and outgoing rates yields a net accumulation rate within the compartment. The free (unbound) concentration of drug leaving a compartment is assumed to equal (is in equilibrium with) the free concentration within that compartment.

This assumption may not be valid for a compartment that is a combination of blood and tissue and is highly perfused (such as viscera). If the drug does not diffuse into and out of the tissue at a rate faster than the transport by blood flow, the assumption also is not correct. Hence, the viscera might be described more accurately as a viscera tissue compartment and a viscera blood compartment. Furthermore, an equation (statement of material balance) written for one compartment contains concentration values from other compartments and, therefore, all compartment equations are interdependent (as are the body functions they describe) and must be solved together.

The venous blood pool compartment is given first, and the terms are
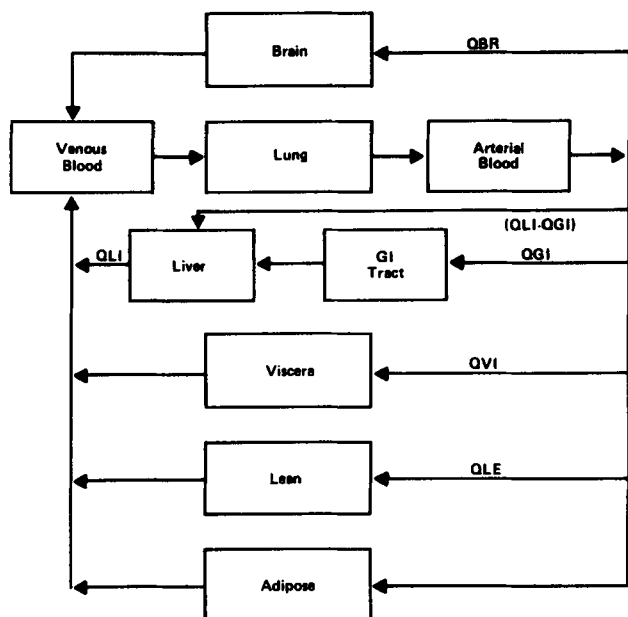
Figure 1—*Body compartments important in procaine distribution.*

elucidated for better understanding of the entire model before stating the other compartment equations.

Venous Blood: Compartment 1—

$$TRAPC(HMT)V_{Vb}F_{W,e}\frac{dC_{Vb}}{dt} + (1 - HMT)V_{Vb}F_{W,Pl}\frac{dC_{Vb}}{dt}$$

$$+ (1 - HMT)V_{Vb}C_{M,Pl}\frac{dX_{Vb}}{dt} = Q_{BR}[TRAPC(HMT)F_{W,e}C_{BR}$$

$$+ (1 - HMT)(F_{W,Pl}C_{BR} + C_{M,Pl}X_{BRb})] + Q_{LI}[TRAPC(HMT)F_{W,e}C_{LI}$$

$$+ (1 - HMT)(F_{W,Pl}C_{LI} + C_{M,Pl}X_{LIb})] + Q_{VI}[TRAPC(HMT)F_{W,e}C_{VI}$$

$$+ (1 - HMT)(F_{W,Pl}C_{VI} + C_{M,Pl}X_{VIb})] + Q_{LE}[TRAPC(HMT)F_{W,e}C_{LE}$$

$$+ (1 - HMT)(F_{W,Pl}C_{LE} + C_{M,Pl}X_{LEb})] + Q_{AD}[TRAPC(HMT)F_{W,e}C_{AD}$$

$$+ (1 - HMT)(F_{W,Pl}C_{AD} + C_{M,Pl}X_{ADb})] - Q[TRAPC(HMT)F_{W,e}C_{Vb}$$

$$+ (1 - HMT)(F_{W,Pl}C_{Vb} + C_{M,Pl}X_{Vb})] - (1 - HMT)V_{Vb}R_{MET,b}$$

$$+ Q_{INF}(BWT) \quad \text{(Eq. 1)}$$

where:

C_i = free (unbound concentration in compartment i) water (micromoles per liter)
Vb = venous blood
LE = lean
AD = adipose
VI = viscera
BR = brain
Ab = arterial blood
LI = liver
LG = lung
e = erythrocyte
Pl = plasma
Q = blood flow rate (liters per minute)
V = volume of the compartment (liters)
HMT = hematocrit of erythrocyte (fraction)
$C_{M,Pl}$ = effective plasma binding protein concentration (kilograms per liter)
$F_{W,Z}$ = fraction water in compartment Z
X = bound concentration (micromoles per kilogram of protein)
$R_{MET,b}$ = metabolism [hydrolysis rate, micromoles per liter (plasma)-minutes]
Q_{INF} = infusion rate [micromoles per kilogram (body)-minutes]
BWT = body mass (kilograms)
$TRAPC$ = ion-trapping constant

Since a compartment contains "free" and "bound" concentrations of drug, summation of these concentrations gives the total concentration. In general, the free drug is assumed to be in the water phase of the compartment, and the bound drug exists in physical attachment to protein or large macromolecules. However, not all protein is effective or available

for binding. Therefore, an effective protein concentration as described previously (9) is used to determine the bound drug concentration. The total concentration for a compartment is described as:

$$C_{tot} = F_{W,Z}C + C_{M,Z}X \quad \text{(Eq. 2)}$$

where:

C_{tot} = total concentration (micromoles per liter)
C = free concentration (micromoles per liter)
X = bound concentration (micromoles per liter)
$F_{W,Z}$ = fraction water (W) in region Z
$C_{M,Z}$ = effective protein macromolecule (M) concentrations (kilograms of protein per liter)

For the venous plasma pool, the total plasma drug concentration is of the form:

$$C_{Pl} = F_{W,Pl}C_{Vb} + C_{M,Pl}X_{Vb} \quad \text{(Eq. 3)}$$

However, for total blood, the amount sequestered within the erythrocytes must be included (10). Due to the erythrocyte ion-trapping effect at a slightly lower intracellular pH (erythrocyte water, pH 7.26) as opposed to extracellular medium pH (plasma water, pH 7.40), the concentration ratio can be calculated as:

$$TRAPC = \frac{C_{eW}}{C_{PW}} = \frac{1 + 10^{pKa \cdot pH_{eW}}}{1 + 10^{pKa \cdot pH_{PW}}} \quad \text{(Eq. 4)}$$

where:

C = free concentration (micromoles per liter)
pKa = negative logarithm of acid dissociation constant
 = 8.92 (procaine base)
eW = erythrocyte water
PW = plasma water

The calculation yields a concentration ratio, C_{eW}/C_{PW} = 1.37. However, a study (11) of procaine uptake in human platelets, although they are smaller than erythrocytes, showed that the highest concentration ratio occurred at pH 7.4 with C_{medium} = 100 mg/liter and was 2.85 ± 0.78. High uptake also was found (12) for several anilide-type local anesthetics. Therefore, it could be concluded that binding was present, but no definitive binding relationship was noted other than a dependence on pH. Hence, in this work, the concentration ratio is only calculated from the ion-trapping effects as per Eq. 4. Additionally, since no difference in uptake was reported (12) from 5 min to 24 hr, a rapid establishment of equilibrium may be assumed.

The drug concentration in erythrocytes as a fraction of blood is determined from the hematocrit (HMT), the erythrocyte water fraction ($F_{W,e}$), the trapping ratio ($TRAPC$), and the plasma water concentration. Combination of the erythrocyte concentration with the total plasma concentration gives the total blood concentration:

$$C_{t,VB} = TRAPC(HMT)F_{W,e}C_{Vb}$$
$$+ (1 - HMT)(F_{W,Pl}C_{Vb} + C_{M,Pl}X_{Vb}) \quad \text{(Eq. 5)}$$

The protein or macromolecular drug binding has a major influence on the concentration relationship (12, 13). The general form for the relationship is:

$$r = \sum_{i=1}^{n} \frac{N_i K_i C}{1 + K_i C} \quad \text{(Eq. 6)}$$

where:

r = moles of bound drug per mole of protein macromolecule (moles per mole of protein)
N_i = average number of type i binding sites per protein macromolecule (moles per mole of protein)
K_i = intrinsic association constant of type i binding site (liters per mole)

A bound concentration of micromoles bound per kilogram of macromolecule is used instead of a mole per mole basis, and the general form of the relationship can be simplified to only one binding site. Therefore:
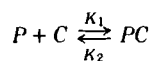
$$X = \frac{BKC}{1 + KC} \quad \text{(Eq. 7)}$$

where:

X = bound concentration (micromoles per kilogram)
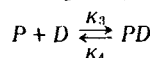C = free concentration (micromoles per liter)

B = binding site constant (micromoles per kilogram)
K = intrinsic association constant (liters per micromole)

This relationship is sufficient in the presence of a single drug. The presence of two or more drugs may cause competition for a binding site, and the equation describing the binding relationship must take this competitive binding into account (14). The following describes the competition between two drugs for a single site on the protein complex:

$$P + C \underset{K_2}{\overset{K_1}{\rightleftharpoons}} PC$$

Scheme I

$$K_c = \frac{K_1}{K_2} = \frac{(PC)}{(P)(C)}$$
(Eq. 8a)

$$P + D \underset{K_4}{\overset{K_3}{\rightleftharpoons}} PD$$

Scheme II

$$K_D = \frac{K_3}{K_4} = \frac{(PD)}{(P)(D)}$$
(Eq. 8b)

$$r = \frac{(PC)}{(P)} = \frac{N_C K_C C}{1 + K_D D + K_C C}$$
(Eq. 9)

and:

$$X = \frac{B_C K_C C}{1 + K_D D + K_C C}$$
(Eq. 10)

where:

B_C = binding site constant for drug C (micromoles per kilogram)
K_C = intrinsic association constant for drug C (liters per micromole)
C = free drug C concentration (micromoles per liter)
D = free inhibitor drug D concentration (micromoles per liter)

The use of the binding equation requires an estimation of the inhibitor drug concentration. A one-compartment model approximation via exponential decay of the initial concentration may be sufficient if the inhibitor drug has a half-life much longer than the drug of interest. In this case, the inhibitor drug concentration changes relatively slowly and can be assumed to act in one compartment uniformly throughout the body. Hence, thiamylal, an ultrashort-acting barbiturate having a half-life of at least 2 hr, which is much longer (~20 times) than that of procaine, was handled as a one-compartment drug in this study. In the clinical situation being simulated, thiamylal is given several minutes before procaine so the equation describing the thiamylal concentration would be:

$$C_{th} = C_{th_0} \exp \frac{-(T + TD)0.693}{T^{1/2}}$$
(Eq. 11)

where:

C_{th} = thiamylal concentration (micromoles per liter)
$C_{th_0} = D_{th}/V_{th}$ = initial concentration
D_{th} = dose (micromoles per kilogram)
V_{th} = volume of distribution (liters per kilogram)
TD = time delay between thiamylal and procaine administration

Another important function of the blood pool with regard to procaine is the metabolism via circulating enzymes, procainesterases (assumed to be plasma cholinesterases). The reaction rate has been well investigated (15–17) and is suited to description by the Michaelis–Menten-type equation of the form:

$$R_{MET} = \frac{V_{max}C}{C_{half} + C}$$
(Eq. 12)

where:

R_{MET} = reaction rate [micromoles per liter (plasma)-minutes]
V_{max} = maximum reaction rate (micromoles per liter-minutes)
C_{half} = free drug concentration (micromoles per liter)

As with protein binding competition, it is necessary to account for the inhibition or competitive effect of other drugs, particularly in the clinical setting where many drugs are administered concurrently. In this work, one such drug of special significance is succinylcholine, a muscle relaxant, which is metabolized by the plasma cholinesterases (18). The derivation and design of the competitive inhibition phenomena for a chemical re-

action are almost identical to those for protein binding, differing only in the final form of the equation. The Michaelis–Menten equation becomes:

$$R_{MET} = \frac{V_{max}C}{C_{half}\left(1 + \frac{I}{K_I}\right) + C}$$
(Eq. 13)

where:

I = free inhibitor concentration (micromoles per liter)
$K_I = K_m$ value or half maximal I concentration (micromoles per liter)

Obviously, the inhibitor increases the value of C_{half}.

Calculation of the final reaction rate requires estimation of the drug I concentration, which in this case is succinylcholine (suxamethonium) (17). Since succinylcholine is very water soluble and sparingly soluble in organic media, it will be assumed that the distribution volume is approximately equal to the extracellular fluid volume. If the intravenously administered dose is eliminated solely by its reaction with plasma cholinesterase, the succinylcholine concentration can be estimated as follows:

$$CSD = \frac{dose - \dfrac{VSD(CSD)T}{CKSD(1 - C/C_{half}) + CSD}(1 - HMT)V_b}{V_{EX}}$$
(Eq. 14)

where:

CSD = free concentration of succinylcholine (micromoles per liter)
VSD = maximum reaction rate [micromoles per liter (plasma)-minutes]
$CKSD$ = K_m value for succinylcholine (micromoles per liter)
V_{EX} = extracellular fluid volume (liters)
V_b = blood volume (liters)
HMT = hematocrit
C = free procaine concentration (micromoles per liter)
C_{half} = K_m value for procaine (micromoles per liter)
dose = intravenous succinylcholine dose (micromoles)
T = time (minutes)

Essentially, the complexity of this model is exhibited in the blood equation. However, the various tissue compartments must be described with particular emphasis on the tissue macromolecular drug binding. Since no literature description of a relationship as a function of free concentration is available for tissue, the plasma binding relationship parameter was assumed to be valid. It remained to determine the effective tissue macromolecule concentration. Values for the partitioning of drug into tissue from plasma are available (10, 19–21). A tissue–plasma partition ratio can be calculated for brain, as an example, as follows:

$$P_{BR} = \frac{F_{W,BRt}C_{BR} + C_{M,BRt}X_{BRt}}{F_{W,Pl}C_{BR} + C_{M,Pl}X_{BRb}} = \frac{plasma}{tissue}$$
(Eq. 15)

The unknown value of $C_{M,BRt}$ (effective macromolecule concentration in brain tissue) can be determined since $F_{W,BRt}$ is available from the literature and the other terms have been previously determined. A slightly different approach to the formulation is needed to handle adipose tissue where the fatty tissue concentration may be approximated by using a Henry's law relationship (21):

$$X_{ADt} = B_{ADt}C_{AD}$$
(Eq. 16)

where B_{ADt} is Henry's law constant for procaine. Hence, the partition equation becomes:

$$P_{AD} = \frac{F_{W,ADt}C_{AD} + C_{M,ADt}B_{ADt}C_{AD}}{F_{W,Pl}C_{AD} + C_{M,Pl}X_{ADb}}$$
(Eq. 17)

Even if B_{ADt} is not known, the combination $C_{M,Adt}B_{ADt}$ is sufficient for the descriptive equation since X_{ADb} in the plasma is calculated from Eq. 10. Now the other compartments can be expressed quantitatively.

Lean: Compartment 2—

$$TRAPC(HMT)V_{LEb}F_{W,e}\frac{dC_{LE}}{dt} + (1 - HMT)V_{LEb}F_{W,Pl}\frac{dC_{LE}}{dt}$$

$$+ (1 - HMT)V_{LEb}C_{M,Pl}\frac{dX_{LEb}}{dt} + V_{LEt}F_{W,LEt}\frac{dC_{LE}}{dt}$$

Table 1—Model Parameters for Standard 70-kg Man [a]

Parameter	Arterial Blood	Venous Blood	Brain	Viscera	Liver	Lean	GI Tract	Adipose	Lung
Tissue volume, liters	—	---	1.50	0.64	1.50	3.92	1.50	12.2	0.60
Flow rate, liters/min	5.54	5.54	0.76	1.66	1.58	1.28	1.20	0.26	5.54
Fraction water	0.714	0.94	0.76	0.78	0.73	0.77	0.74	0.19	0.90
Blood volume, liters	0.58	1.16	0.47	1.05	0.37	0.52	1.05	0.16	0.46

[a] Values modified from Refs. 22 and 25.

$$+ V_{LEt}C_{M,LEt} \frac{dX_{LEt}}{dt} = Q_{LE}[TRAPC(HMT)F_{w,e}C_{Vb}$$
$$+ (1 - HMT)(F_{w,Pl}C_{Vb} + C_{M,Pl}X_{Vb})$$
$$- TRAPC(HMT)F_{w,e}C_{LE}$$
$$+ (1 - HMT)(F_{w,Pl}C_{LE} + C_{M,Pl}X_{LEb})]$$
$$- (1 - HMT)V_{LEb}R_{MET,LEb} \quad (Eq.\ 18)$$

Adipose: Compartment 3—

$$TRAPC(HMT)V_{ADb}F_{w,e} \frac{dC_{AD}}{dt} + (1 - HMT)V_{ADb}F_{w,Pl}$$
$$\times \frac{dC_{AD}}{dt} + (1 - HMT)V_{ADb}C_{M,Pl} \frac{dX_{ADb}}{dt}$$
$$+ V_{ADt}F_{w,ADt} \frac{dC_{AD}}{dt} + V_{ADt}C_{M,ADt} \frac{dX_{ADt}}{dt}$$
$$= Q_{AD}[TRAPC(HMT)F_{w,e}C_{Vb} + (1 - HMT)(F_{w,Pl}C_{Vb}$$
$$+ C_{M,Pl}X_{Vb}) - TRAPC(HMT)F_{w,e}C_{AD}$$
$$+ (1 - HMT)(F_{w,Pl}C_{AD} + C_{M,Pl}X_{ADb})]$$
$$- (1 - HMT)V_{ADb}R_{MET,ADb} \quad (Eq.\ 19)$$

Because of the highly perfused nature of the brain, heart, and kidneys as well as some other organs, the assumption that mass transfer with each compartment is flow limited, i.e., at the normal blood flow rate, incoming drug is instantly mixed with surrounding tissue and the outgoing free drug concentration is equal to the total compartment free concentration, should be considered. For high lipid-soluble drugs, this assumption is valid; but for less soluble ones, it is not. This subject is treated thoroughly in the literature (5–7).

Instead of a transfer coefficient equal to infinity, a transfer value for procaine equal to the flow rate of the compartment could be used for lack of a more exact determination. It is significant to account for this phenomenon since the rate of procaine appearance into cerebrospinal fluid is less than the ratio of blood flow to tissue volume (19). Conversely, in the lean and adipose compartments, the flow to volume ratio is much less than the transfer rate into tissue, and the uniformity is still assumed to be valid.

The viscera, brain, liver, GI tract, and lung compartments could be described with plasma and tissue separated, where the transfer between plasma and tissue is dependent on the free concentration difference. However, the following description ignores the finite plasma–tissue transfer and combines plasma and tissue into one compartment for simplicity.

Viscera: Compartment 4—

$$TRAPC(HMT)V_{Vlb}F_{w,e} \frac{dC_{VI}}{dt} + (1 - HMT)V_{Vlb}F_{w,Pl}$$
$$\times \frac{dC_{VI}}{dt} + (1 - HMT)V_{Vlb}C_{M,Pl} \frac{dX_{VI}}{dt}$$
$$+ V_{Vlt}F_{w,Vlt} \frac{dC_{Vlb}}{dt} + V_{Vlt}C_{M,Vlt} \frac{dX_{Vlb}}{dt}$$
$$= Q_{VI}[TRAPC(HMT)F_{w,e}C_{Ab} + (1 - HMT)(F_{w,Pl}C_{Ab}$$
$$+ C_{M,Pl}X_{Ab}) - TRAPC(HMT)F_{w,e}C_{Vlb}$$
$$+ (1 - HMT)(F_{w,Pl}C_{Vlb} + C_{M,Pl}X_{Vlb})]$$
$$- (1 - HMT)V_{Vlb}R_{MET,Vlb} - RC(C_{Vlb}) \quad (Eq.\ 20)$$

where RC is the renal clearance rate (liters per minute).

Brain: Compartment 5—

$$TRAPC(HMT)V_{BRb}F_{w,e} \frac{dC_{BR}}{dt} + (1 - HMT)V_{BRb}F_{w,Pl}$$
$$\times \frac{dC_{BR}}{dt} + (1 - HMT)V_{BRb}C_{M,Pl} \frac{dX_{BRb}}{dt}$$

$$+ V_{BRt}F_{w,BRt} \frac{dC_{BR}}{dt} + V_{BRt}C_{M,BRt} \frac{dX_{BRt}}{dt}$$
$$= Q_{BR}[TRAPC(HMT)F_{w,e}C_{Ab} + (1 - HMT)(F_{w,Pl}C_{Ab}$$
$$+ C_{M,Pl}X_{Ab}) - TRAPC(HMT)F_{w,e}C_{BR}$$
$$+ (1 - HMT)(F_{w,Pl}C_{BR} + C_{M,Pl}X_{BR})]$$
$$- (1 - HMT)V_{BRb}R_{MET,BRb} \quad (Eq.\ 21)$$

Liver: Compartment 6—

$$TRAPC(HMT)V_{Llb}F_{w,e} \frac{dC_{LI}}{dt} + (1 - HMT)V_{Llb}F_{w,Pl} \frac{dC_{LI}}{dt}$$
$$+ (1 - HMT)V_{Llb}C_{M,Pl} \frac{dX_{Llb}}{dt} + V_{Llt}F_{w,Llt} \frac{dC_{LI}}{dt}$$
$$+ V_{Llt}C_{M,Llt} \frac{dX_{Llt}}{dt} = (Q_{LI} - Q_{GI}) [TRAPC(HMT)F_{w,e}C_{Ab}$$
$$+ (1 - HMT)(F_{w,Pl}C_{Ab} + C_{M,Pl}X_{Ab})]$$
$$+ Q_{GI}[TRAPC(HMT)F_{w,e}C_{GI} + (1 - HMT)(F_{w,Pl}C_{GI}$$
$$+ C_{M,Pl}X_{Glb})] - Q_{LI}[TRAPC(HMT)F_{w,e}C_{LI}$$
$$+ (1 - HMT)(F_{w,Pl}C_{LI} + C_{M,Pl}X_{Llb})]$$
$$- (1 - HMT)V_{Llb}R_{MET,Llb}$$
$$- (V_{Llt}R_{Llt}C_{Llb})/(C_{half} + C_{Llb}) \quad (Eq.\ 22)$$

where R_{Llt} is the reaction rate constant for liver metabolism of procaine (minutes^{-1}).

GI Tract: Compartment 7—

$$TRAPC(HMT)V_{Glb}F_{w,e} \frac{dC_{GI}}{dt} + (1 - HMT)_{Glb}F_{w,Pl} \frac{dC_{GI}}{dt}$$
$$+ (1 - HMT)V_{Glb}C_{M,Pl} \frac{dX_{Glb}}{dt} + V_{Glt}F_{w,Glt} \frac{dC_{GI}}{dt}$$
$$+ V_{Glt}C_{M,Glt} \frac{dX_{Glt}}{dt} = Q_{GI}\{TRAPC(HMT)F_{w,e}C_{Ab}$$
$$+ (1 - HMT)(F_{w,Pl}C_{Ab} + C_{M,Pl}X_{Ab}) - TRAPC(HMT)F_{w,e}C_{Glb}$$
$$+ (1 - HMT)(F_{w,Pl}C_{Glb} + C_{M,Pl}X_{Glb})\}$$
$$- (1 - HMT)V_{Glb}R_{MET,Glb} \quad (Eq.\ 23)$$

Lungs: Compartment 8—

$$TRAPC(HMT)V_{LGb}F_{w,e} \frac{dC_{LG}}{dt} + (1 - HMT)V_{LGb} \frac{dC_{LG}}{dt}$$
$$+ (1 - HMT)V_{LGb}C_{M,Pl} \frac{dX_{LGb}}{dt} + V_{LGt}F_{w,LGt} \frac{dC_{LG}}{dt}$$
$$+ V_{LGt}C_{M,LGt} \frac{dX_{LGt}}{dt} = Q_b[TRAPC(HMT)F_{w,e}C_{Vb}$$
$$+ (1 - HMT)(F_{w,Pl}C_{Vb} + C_{M,Pl}X_{Vb}) - TRAPC(HMT)F_{w,e}C_{LG}$$
$$+ (1 - HMT)(F_{w,Pl}C_{LG} + C_{M,Pl}X_{LGb})]$$
$$- V_{LGb}(1 - HMT)R_{MET,LGb} \quad (Eq.\ 24)$$

Arterial Blood: Compartment 9—

$$TRAPC(HMT)V_{Ab}F_{w,e} \frac{dC_{Ab}}{dt} + (1 - HMT)V_{Ab}F_{w,Pl} \frac{dC_{Ab}}{dt}$$
$$+ (1 - HMT)V_{Ab}C_{M,Pl} \frac{dX_{Ab}}{dt} = Q_B[TRAPC(HMT)F_{w,e}C_{LG}$$
$$+ (1 - HMT)(F_{w,Pl}C_{LG} + C_{M,Pl}X_{LGb}) - TRAPC(HMT)F_{w,e}C_{Ab}$$
$$+ (1 - HMT)(F_{w,Pl}C_{Ab} + C_{M,Pl}X_{Ab})]$$
$$- (1 - HMT)V_{Ab}R_{MET,Ab} \quad (Eq.\ 25)$$

The physiological and anatomical parameters were based on those of a standard 70-kg man but were scaled, to simulate each individual studied, on the basis of basal energy metabolism (BEM) which is a
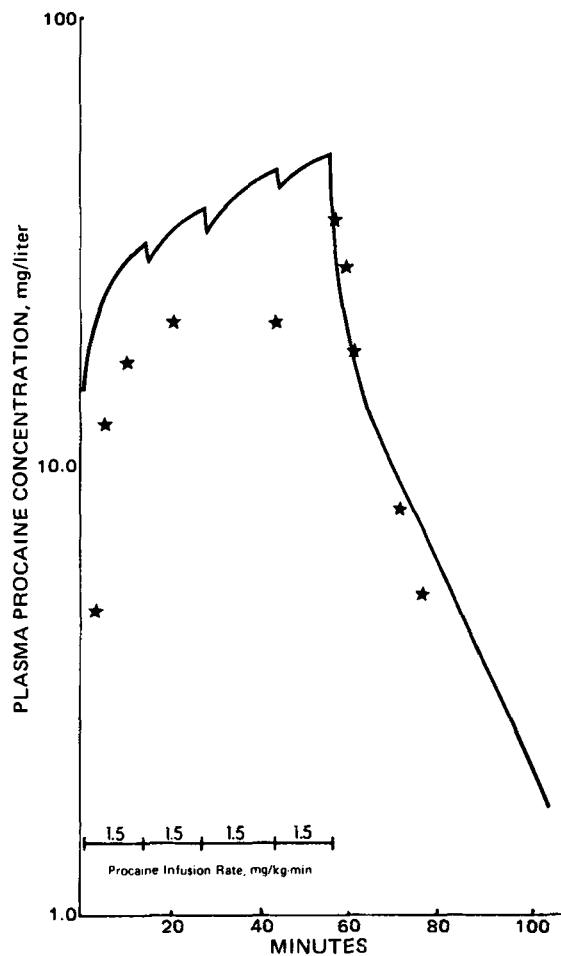
Figure 2—*Model predictions of plasma procaine concentrations versus experimental results for a female (age 34, weight 58.7 kg, height 177.8 cm, and hematocrit 35.0) with infusion rates and duration as shown.*
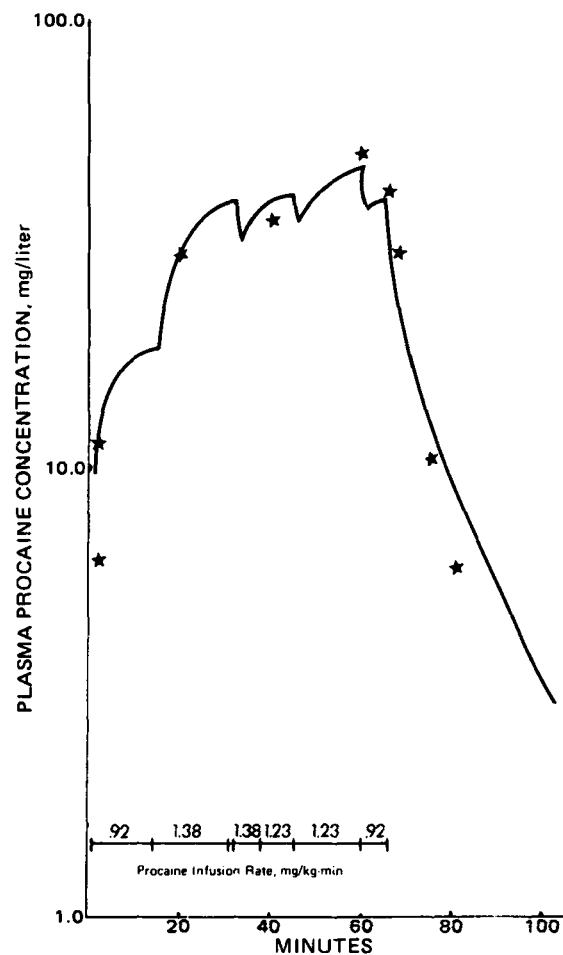

Figure 3—*Model predictions of plasma procaine concentrations versus experimental results for a female (age 24, weight 65 kg, height 165 cm, and hematocrit 36.8) with infusion rates and duration as shown.*

function of age, sex, height, and weight. This value was estimated by calculating the body surface area as:

$$S = 0.007184 \ (Wt^{0.425})(Ht^{0.725}) \qquad \text{(Eq. 26)}$$

where Wt is weight (kilograms) and Ht is height (centimeters). Then, based on the tables relating age, surface area, and basal energy metabolism (22), for males 18–25 years:

$$BEM = [40.5 - (age - 18) \times 0.3](S)/60 \qquad \text{(Eq. 27a)}$$

for males over 25 years:

$$BEM = [38.4 - (age - 25) \times 0.11](S)/60 \qquad \text{(Eq. 27b)}$$

for females 20–40 years:

$$BEM = [35.3 - (age - 20) \times 0.05](S)/60 \qquad \text{(Eq. 27c)}$$

and for females over 40 years:

$$BEM = [34.3 - (age - 40) \times 0.10](S)/60 \qquad \text{(Eq. 27d)}$$

The fraction fat can be estimated from the tables (22) by:

$$FRFAT = 1.04 + 0.4 \ (Wt - 50)/30 - BEM \qquad \text{(Eq. 28)}$$

Since the standard 70-kg man is considered to contain approximately 17.4% fat, the anatomical scaling was based on the body weight minus the fat contents by:

$$ANA = Wt(1 - FRFAT)/57.8 \qquad \text{(Eq. 29)}$$

where ANA is the scale factor.

RESULTS AND DISCUSSION

Analytical solution of the simultaneous differential equations was not

feasible because of the nonlinearities caused by the binding terms. Therefore, the equations were solved by the fourth-order Runge–Kutta numerical method. The model stability was tested by comparing the numerical results from the standard values in Tables I and II with those from variations of the standard value for each of the following parameters:

1. ±10% variation of the volume of any body region
2. ±10% variation of the volume and the blood flow rate of any body region
3. ±10% variation of the water volume fraction of any body region
4. ±10% variation of the lipid solubility constant, BAT
5. ±10% of the binding constant, B
6. ±10% of the metabolism constants, VSD and C_{half}
7. ±10% variation of the effective binding macromolecule concentration of any body region

Figures 2 and 3 compare the model simulation with experimental values for two cases with a wide variation of physiological parameters as well as different infusion rates. The model was designed to account for both variations in the infusion rate and interruptions in the infusion continuity. This flexibility permitted a close simulation of the actual clinical application of the procaine infusion. As shown in the figures, due to rapid procaine hydrolysis in the blood, the rapid decline in concentration resulting from very short interruptions in the infusion can be very pronounced and will result in a substantial error in the simulated prediction of the concentration if it is not accounted for in the model design.

Figure 2 shows the experimental kinetic data of plasma procaine levels (symbol) and the model-predicted kinetics (solid line) for a 1.5-mg/kg/min intravenous infusion in a female. The results are in agreement within the range of measurement accuracy of the experimental data. Similar results are shown in Fig. 3 for a varied infusion rate in a female.

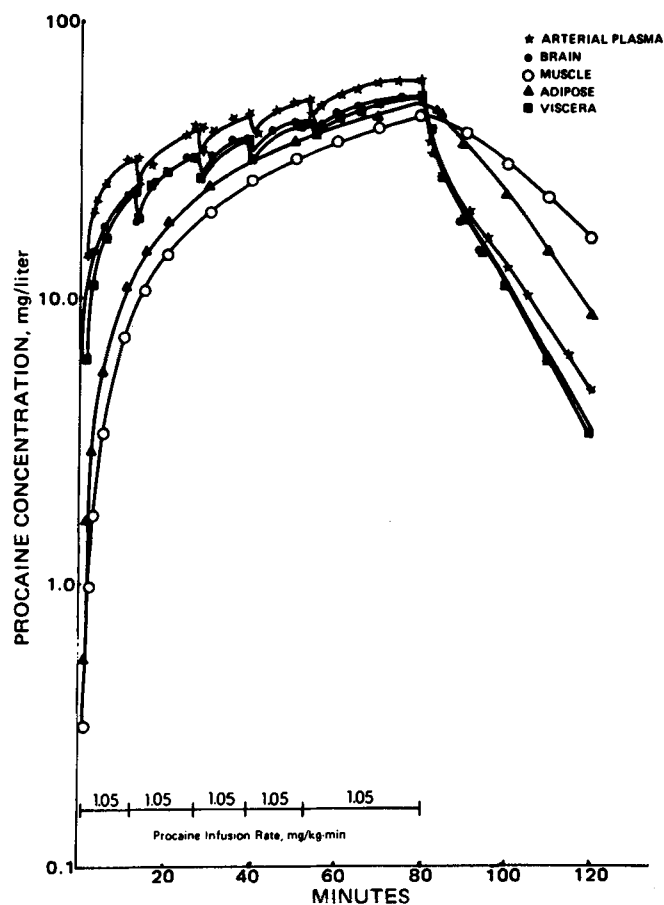Figure 4 demonstrates the predicted procaine concentrations in the

Figure 4—*Model predictions for various compartments (arterial plasma, brain, viscera, adipose, and muscle) for a female (age 25, weight 87.4, height 165 cm, and hematocrit 35.3) with infusion rates and duration as shown.*
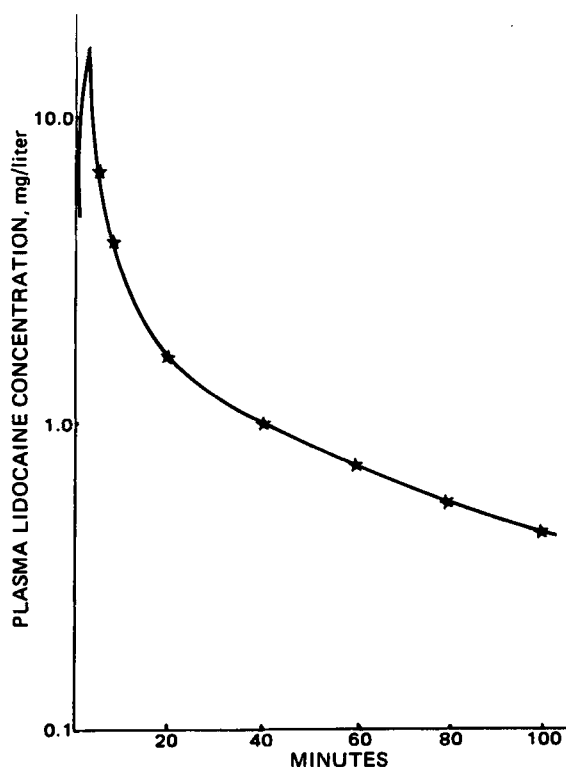

Figure 5—*Model predictions of plasma lidocaine concentrations versus literature values (12).*

Table II—Binding and Metabolism Parameters

Parameter	Procaine	Lidocaine[a]
Effective binding macromolecule concentration, kg/liter		
Brain	0.00079[b]	0.00135
Plasma	0.000945[b]	0.000945
Liver	0.0115[b]	0.000485
GI tract	0.0142[b]	0.00319
Viscera	0.0115[b]	0.00233
Lean	0.00167[b]	0.00052
Lung	0.00238[b]	0.00418
Adipose	0.01	0.0481
Binding factors		
Binding site constants, moles/liter	29,500.0[c]	28,571.0
Intrinsic association constant, liters/μmole	0.00314[c]	0.101
pKa	8.92[c]	7.86
Lipid solubility constant	12.0[c]	100.0
Maximum reaction rate, μmoles/liter (plasma)·min	70.0[d]	0.0
Free concentration reaction rate, μmoles/liter	28.0[d]	6.0
Renal clearance, liters/min	0.2	0.1

[a] Calculated based on Refs. 12 and 23. [b] Calculated based on Ref. 19. [c] Calculated based on Refs. 13 and 23. [d] Calculated based on Ref. 16.

various body regions for an infusion rate of 1.05 mg/kg/min. Since it was not possible to analyze samples from body regions other than the blood compartments, the basic model was further tested using literature data for lidocaine infusions (1, 20). With the appropriate lidocaine parameters (Table II), several simulations were made (one is shown in Fig. 5). The results of the simulation kinetics and the experimental kinetics are very similar and thus indicate the accuracy of the basic model.

CONCLUSIONS

Knowledge of the kinetic behavior of a drug in blood or plasma may not provide sufficient information for appropriate therapy; additional kinetic information of drug levels in specific organs, tissues, or body regions may be required for the development of improved dosage regimens. The pharmacokinetic model presented can predict detailed distribution in humans of intravenous infusion of local anesthetics, procaine and lidocaine, not only in blood or plasma but also in brain, liver, and other tissues or body regions.

Based on a general perfusion model, this model relates individual characteristics such as sex, age, weight, height, infusion rate, and hematocrit to general parameters such as metabolism, protein binding, ion-trapping effects, and tissue–plasma distribution coefficients to provide an individualized distribution prediction. Since each equation (compartment) in the system contains terms (concentrations) from other compartments and, therefore, all equations are interdependent, changes in any compartment influence the other compartments. This feature of the model has an important application in clinical pharmacokinetics.

Experimentally observed kinetics of blood procaine levels collected during procaine intravenous infusion as an adjunct to surgical anesthesia and blood levels of lidocaine obtained from the literature compared very well with the model simulation. While it was not possible in this study to collect experimental data in any organs or tissues other than the blood to support the predicted drug level, information from the literature derived from animal studies of tissue levels tends to verify the accuracy of the model. Until appropriate data for procaine concentrations are available for comparison with the predicted values, the predictions must be considered only to offer an approximation of what the physiological and pharmacological parameters indicate should occur. However, one application of this model is the comparison of drug levels obtained within a body region as a result of different infusion conditions such as rate changes, addition of thiamylal or succinylcholine, and variations in metabolism without the potential drastic effects an individual might experience under the same conditions. As more conditions are tested, the successful predictions should clarify the pharmacokinetics being described.

REFERENCES

(1) G. T. Tucker and R. A. Boas, *Anesthesiology*, **34**, 538 (1971).
(2) M. Ehrnebo, *J. Pharm Sci.*, **63**, 1114 (1974).
(3) D. D. Breimer, *Br. J. Anaesth.*, **48**, 643 (1976).

(4) J. C. K. Loo and S. Riegelman, J. Pharm. Sci., 59, 53 (1970).

(5) K. B. Bischoff, R. L. Dedrick, D. S. Zaharko, and J. A. Longstreth, ibid., 60, 1128 (1971).

(6) K. B. Bischoff and R. L. Dedrick, ibid., 57, 1346 (1968).

(7) K. B. Bischoff and R. L. Dedrick, Chem. Eng. Prog. Symp. Ser., 64, 32 (1968).

(8) R. H. Smith, M. A. Brewster, J. A. MacDonald, and D. S. Thompson, Clin. Chem., 24, 1599 (1978).

(9) D. Shen and M. Gibaldi, J. Pharm. Sci., 63, 1698 (1974).

(10) L. S. Schanker, P. A. Nafpliotis, and J. M. Johnson, J. Pharmacol. Exp. Ther., 133, 325 (1961).

(11) H. M. Soloman and P. D. Zieve, ibid., 155, 112 (1967).

(12) G. T. Tucker, R. N. Boyes, P. O. Bridenbough, and D. C. Moore, Anesthesiology, 33, 287 (1970).

(13) V. S. Sawinski and G. W. Rapp, J. Dental Res., 42, 1429 (1963).

(14) A. Goldstein, L. Aronaw, and S. M. Kalman, "The Basis of Pharmacology," 2nd ed., Wiley, New York, N.Y., 1974.

(15) B. B. Brodie, P. A. Lief, and R. Poet, J. Pharmacol. Exp. Ther.,

94, 359 (1948).

(16) W. Kalow, ibid., 104, 122 (1952).

(17) N. Kvisselgaard and F. Moya, Acta Anaesth. Scand., 5, 1 (1961).

(18) L. B. Hersh, P. P. Raj, and D. Ohlweiler, J. Pharmacol. Exp. Ther., 189, 544 (1974).

(19) J. E. Usubiaga, F. Moya, J. A. Wikinski, R. Wikinski, and L. E. Usubiaga, Br. J. Anaesth., 39, 943 (1967).

(20) J. B. Keenaghan and R. N. Boyes, J. Pharmacol. Exp. Ther., 180, 454 (1972).

(21) J. Buchi and X. Perlia, "International Encyclopedia of Pharmacology and Therapeutics," sect. 8, vol. 1, Pergamon, Elmsford, N.Y., 1971, chaps. 1, 2, 5, 39.

(22) W. S. Spector, "Handbook of Biological Data," Saunders, Philadelphia, Pa., 1956.

(23) C. Sung and A. P. Truant, J. Pharmacol. Exp. Ther., 112, 432 (1954).

(24) A. P. Truant and B. Takman, Anesth. Anal., 38, 478 (1959).

(25) W. W. Mapleson, J. Appl. Physiol., 18, 197 (1963).

Myoinositol Uptake by Rat Hepatocytes *In Vitro*

CHI-PO CHEN [x] and VAN T. VU

Abstract □ Myoinositol uptake by rat hepatocytes *in vitro* was studied. Adult rat hepatocytes were prepared by digestion of the perfused liver with collagenase. Cell suspensions were incubated with tritium-labeled myoinositol in pH 7.4 Krebs bicarbonate solution containing 1% gelatin at 37°. ^{14}C-Carbon-labeled polyethylene glycol was used as a marker of adherent extracellular fluid volume. Myoinositol uptake was demonstrable after 5 min of incubation, but no intracellular concentration in excess of that in the incubation medium was observed after 60 min of incubation. Uptake saturation over a wide myoinositol concentration range could not be demonstrated. Neither the omission of sodium ions nor the inclusion of ouabain suppressed the distribution ratio significantly. Metabolic inhibitors and lower temperatures also showed no effect. Hexoses, phlorizin or mannitol, exerted no observable effect on myoinositol uptake. The results indicated that myoinositol uptake by rat hepatocytes is probably a passive process.

Keyphrases □ Myoinositol—uptake by hepatocytes, *in vitro*, rats, pharmacokinetics □ Hepatocytes—myoinositol uptake, pharmacokinetics, *in vitro*, rats □ Liver—myoinositol uptake, *in vitro*, pharmacokinetics, rats

myoinositol can be utilized in β-lipoprotein production in the endoplasmic reticulum. The newly synthesized β-lipoprotein is transported from the liver to the blood (4). In addition, exogenous myoinositol inhibits any further deposition of either liver triglycerols or cholesterol and causes the removal of the lipids deposited during the myoinositol-deficiency period (5–7).

Although there is much evidence that myoinositol is transported into the small intestine (8), kidney (9–12), central nervous system (13–16), and crystalline lens (17–19) *via* a specific carrier-mediated system, hepatic uptake of myoinositol has not been studied in spite of its well-known lipotropic activity. Hauser (11) reported that the radioactive myoinositol distribution ratio in liver slices is less than one-half of the radioactivity in the incubation medium, while the hepatic myoinositol concentration *in vivo* is similar to that of plasma; higher hepatic than blood myoinositol concentrations also were observed (20, 21).

In recent years, the use of isolated hepatocytes for various biochemical and pharmacological studies has gained wide acceptance (22). Studies with isolated liver cells can clarify certain molecular aspects of the transport system, such as binding and metabolism, while cellular integrity is maintained.

The purpose of this study was to investigate hepatic myoinositol uptake using liver cells freshly isolated from normal adult rats.

BACKGROUND

Myoinositol has long been considered to be a lipotropic agent because of its ability to prevent and remove fat deposits in the liver (3, 4). This lipotropic action is thought to be due to stimulation of hepatic transferable phosphatidylinositol synthesis. Once formed, the phosphorylated

The liver plays a predominant role in lipid metabolism. Under normal conditions, the influx of nonesterified fatty acids into the liver from the serum is counterbalanced by the formation of lipoprotein, which is transported back to the blood. The whole process requires myoinositol. In myoinositol-deficient animals, fatty livers often can be observed since the rate of fatty acid transport to the liver from the adipose tissue exceeds the capacity of the liver to mobilize the lipid and to transport it back to the plasma (1, 2). The administration of myoinositol to myoinositol-deficient animals often can alleviate the fatty liver condition.

EXPERIMENTAL

Male rats[1], 200–300 g, were housed in groups in wire-bottomed cages in an air-conditioned room (23°). They received regular laboratory chow and water without restriction.

The methods of liver perfusion and cell isolation were described previously (23, 24). Cell viability was determined by the exclusion of 0.2% trypan blue from the cells and was frequently checked by incubating the cells with α-aminoisobutyric acid, which is actively accumulated by the hepatocytes (23). Cell pellets, following the final wash of the isolation procedure, were resuspended in 10 volumes of pH 7.4 Krebs–Ringer bicarbonate buffer containing 1% gelatin.

Uptake studies were performed by placing 5 ml of the final cell suspension (50–80 mg wet weight/ml of suspension) into 25-ml plastic erlenmeyer flasks. Under control conditions, the cell suspensions contained a trace amount of [2-^{3}H(N)]-myoinositol[2] (3 μCi/nmole/100 ml of suspension) with or without 0.1 μmole of nonlabeled myoinositol/ml. In

---

[1] Charles River Breeding Laboratory, Wilmington, Mass.

[2] New England Nuclear Corp., Boston, Mass.